Localized d-d excitations in NiO(100) and CoO(100)

A. Gorschlüter and H. Merz
Physikalisches Institut der Universität Münster, D-48149 Münster, Wilhelm-Klemm-Strasse 10, Germany
(Received 25 October 1993; revised manuscript received 4 February 1994)

The localized character of the $3d$ electrons in the antiferromagnetic oxides NiO(100) and CoO(100) has been studied with electron energy-loss spectroscopy at primary energies between 20 and 1200 eV. The spectra of both charge-transfer compounds exhibit weak but sharp loss structures within the insulating gap region due to crystal-field excitations of the $3d^n$ configuration ($d^n \rightarrow d^{n*}$). These parity forbidden d-d excitations are strongly enhanced at low primary energies due to exchange scattering. Their observed loss intensity depends on the momentum transfer at the scattering process as is shown by angle-dependent measurements. At NiO(100) a surface d state is found that is due to the lower symmetry of the ligand field at the surface. The measurements demonstrate the existence of spin-forbidden exchange excitations $^3A_{2g} \rightarrow (^1E_g, ^1T_{1g})$ in NiO(100) and reveal their excitation energies. A resonant enhancement of all intra-atomic d-d transitions in NiO(100) is found at the Ni $3s$ excitation threshold. Temperature-dependent measurements up to the Néel point show only little influence of the antiferromagnetic ordering on the EELS spectra of NiO(100). The different shapes of the absorption edges due to interatomic d-d transitions across the insulating gaps of NiO(100) and CoO(100) are discussed.

I. INTRODUCTION

The occurrence of localized $3d$ electrons in transition-metal (TM) compounds and the nature of the insulating gap in systems such as NiO have been subjects of many experimental and theoretical studies.[1-5] In the Mott-Hubbard picture[6,7] it is the strong Coulomb interaction between the $3d$ electrons that leads to an energy splitting of the d^n and d^{n+1} states of several eV. As a result the metal $3d$ electrons are localized and charge fluctuations such as $d^n d^n \rightarrow d^{n+1} d^{n-1}$ between adjacent transition-metal sites should determine the gap width. For NiO this picture would lead to a gap width of ≈ 10 eV,[8] which is a value much larger than the experimental values (3.2 eV) derived from optical-absorption[9] and electron energy-loss spectroscopy (EELS) measurements.[10] Better agreement between theory and experiment is achieved when additionally charge transfer between the ligand $2p$ states and the metal $3d$ states is taken into account. In the charge-transfer model a d electron is transferred between two TM sites and, as a result of the large change in the local $3d$ charge density, the d hole is screened by a $p \rightarrow d$ charge transfer. In this picture, it is the process $d^n d^n \rightarrow d^{n+1} d^n L^-$ (L^- denotes a ligand hole) that determines the gap width. In both the Mott-Hubbard picture and the charge-transfer picture *interatomic* transitions are involved in the gap transitions.

However, attempts have also been made to explain the insulating gap of NiO in a delocalized band picture with only one Ni ion involved[11] and it is still a point under discussion whether the low-energy transitions just across the gap are due to excitations involving only one Ni ion or two Ni ions. Another question is, how the two-site transitions can cause the strong rise in intensity at the absorption edge observed in optical-absorption spectroscopy.[12] For clarifying these questions EELS on NiO and CoO can provide new information about the mechanisms.

Because of localized electrons in only partially filled $3d$ shells in NiO and CoO it is also possible to excite low-energy *intra-atomic* transitions between d^n levels. These d^n states are energetically split by the cubic crystal field and the ligand field. In optical-absorption measurements on NiO (Ref. 13,14) and CoO (Ref. 15) the more or less atomiclike transitions between d^n states appear as very weak features because the excitations $d^n \rightarrow d^{n*}$ are forbidden by parity selection rules. Some transitions are additionally forbidden by spin selection rules and cannot—in the absence of spin-orbit interaction—be excited directly with photons. With EELS, however, all states of the d^{n*} configuration can be reached and a determination of excitation energies of transitions changing the multiplicity is possible.

EELS experiments on rare-earth materials show—in analogy to d-d transitions—dipole forbidden transitions between localized $4f$ levels.[16-18] These excitations appear as sharp structures in the spectra. Some of these f-f transitions show a strong dependence on primary energy and scattering geometry, which is presumably due to electron exchange scattering. For the spin-forbidden d-d transitions in NiO and CoO that cannot be excited by direct scattering it is also to be expected that electron exchange scattering contributes to the observed loss intensity in EELS and shows similarities to experiments on rare-earth compounds.

It has been supposed that the intensity of triplet-singlet d-d transitions in NiO depends on the antiferromagnetic ordering of the magnetic moments[19-21] but an investigation of d-d transitions up and below the Néel temperature has not yet been reported.

In this paper, we present an EELS study of UHV-cleaved NiO(100) and CoO(100). Both oxides consist of TM ions with partially filled $3d$ shells octahedrally surrounded by oxygen ions and both exhibit antiferromagnetic ordering of the local magnetic moments below their

Néel temperature. The aim of this paper is to clarify the nature of the low-energy excitations just across the gap, to point out the role of exchange interaction for the intra-atomic *d-d* excitations within the gap and to reveal the influence of the antiferromagnetism on the transition rates.

II. EXPERIMENT

For the EELS measurements we used a Pierce-type electron gun and a simulated hemispherical spectrometer[22] with a four element electron lens. Both components can be rotated around the sample and allow angular-dependent studies with an angular resolution of about 5°. For EELS the primary electron beam was directed onto the sample surface 45° off normal and the acceptance angle was varied. The total experimental energy resolution of the system is 250 meV at a constant pass energy of 30 eV. Since the preparation of stoichiometric single crystalline thin films of NiO and CoO without defect states is a difficult task and the electronic structure in thin films may differ from that in solids, we used for this experiment solid single crystalline samples grown by the Verneuil method.[23] NiO(100) and CoO(100) surfaces were prepared by cleaving the crystals in the UHV chamber at a pressure of 5×10^{-9} Pa. At this pressure also the measurements were carried out. After the cleavage the samples were about 1 mm thick and 10 mm in diameter. They could be cooled down to 100 K or heated to 600 K. The conductivity of most of the NiO samples was sufficient to obtain EELS spectra undistorted by a charging of the sample surface at room temperature (current density of the primary electron beam: 0.02 μA/ mm^2 at 20 eV, spot diameter: 3 mm). CoO crystals at analogous conditions had to be heated to 370 K to prevent sample charging. The samples were additionally characterized by Auger electron spectroscopy and bremsstrahlung isochromat spectroscopy (BIS) measurements.

III. INTERATOMIC TRANSITIONS IN NiO(100) AND CoO(100)

EELS spectra of NiO(100) and CoO(100) measured at different primary energies are shown in Fig. 1. In all figures the position of the elastic peak is indicated by a vertical line. The loss spectrum of NiO(100) exhibits at $E_p=1200$ eV beside the elastic peak a region up to about 3.1 eV with very low loss intensity that characterizes the insulating gap. The following steep rise to feature *B* at 5.0 eV indicates dipole allowed transitions. Now, the first affinity level seen in BIS is a d^9 state at 3.9 eV and the highest occupied states are also of *d* character (d^8, d^8L^-).[8] This would suggest that *d-d* transitions are causing the steep onset, but it is not plausible to explain the strong intensity of feature *B* simply by *d-d* transitions because they are forbidden by dipole selection rules. Although hybridization of Ni 3*d* states with O 2*p* states in the ground state of a NiO cluster must be taken into account for an explanation, it seems that the direct weakening of the dipole selection rules herewith is only marginal, because intra-atomic *d-d* excitations of the same ground state—which should as well be influenced by this

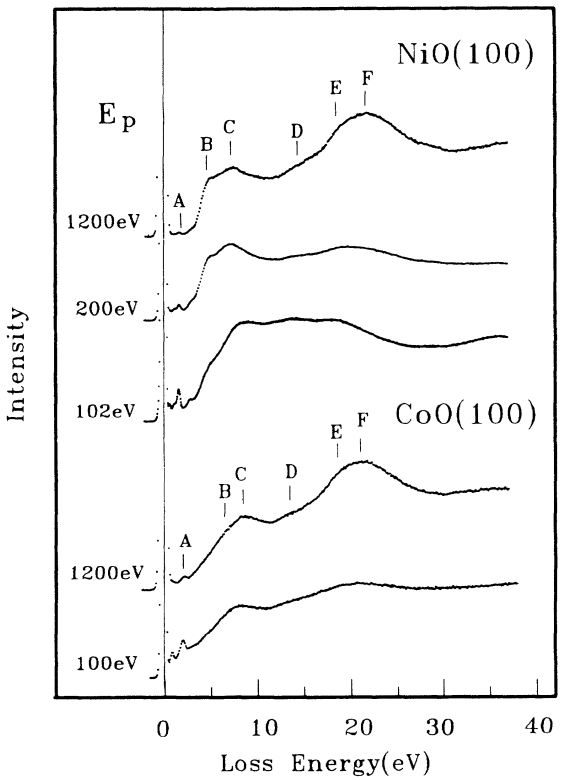

FIG. 1. Dependence of the loss features of NiO(100) and CoO(100) on the primary energy. The spectra were recorded in specular scattering geometry. Zero intensity is for each spectrum indicated by the bottom of the high-energy side of the elastic peak.

hybridization—are suppressed by dipole selection rules and are only barely visible at high primary energies (see Sec. IV). If, however, a *d* electron is removed from one Ni ion and transferred to an adjacent Ni ion, the large change in the local 3*d* charge density is accompanied by strong relaxation processes which result in a screening of the *d* hole by a charge transfer from the local ligand 2*p* orbitals to the metal 3*d* orbitals. These relaxation effects are the reason for strong satellite structures on photoemission spectroscopy (PES) on highly correlated materials. It seems that this relaxation leads to a mixing of *p*- and *d*-wave functions and that, therefore, in a slow experiment such as EELS, transitions between *d* states of adjacent Ni ions can be observed as intense features in the loss spectra. Calculations of the first ionization state in NiO indeed reveal a mixed *p* and *d* character for the hole in the photoionized state.[24] Interatomic transitions from the unscreened d^7 states at about 8-eV binding energy[24,25] to the d^9-final state are not observed in the EELS spectra.

The ground state of Ni^{2+} in NiO has $^3A_{2g}$ symmetry with an electronic configuration $[(t_{2g}\uparrow)^3(e_g\uparrow)^2(t_{2g}\downarrow)^3]$ (Fig. 2). In cluster calculations of electron removal states by Fujimori and Minami[24] the $^4T_{1g}$ state has been found as the first ionization state with the largest spectral weight, whereas calculations of van Elp *et al.*[25] reveal the ^2E_g state as the first electron removal level. In their calculations, however, also the $^4T_{1g}$ state at about 0.5 eV

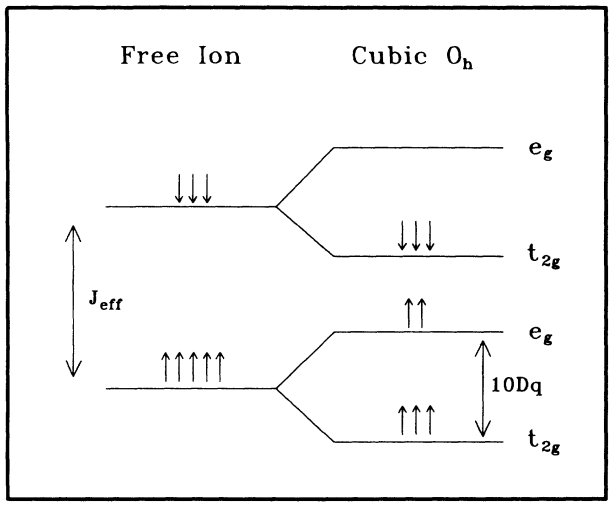

FIG. 2. Schematic diagram of the splitting of the d^8 states of Ni^{2+} in spherical and cubic symmetry due to Hunds-rule exchange (J_{eff}) and ligand field contributions ($10Dq$) in NiO (Ref. 4). Co^{2+} in CoO has one less ($t_{2g}\downarrow$) electron than Ni^{2+} in NiO.

higher binding energy has the largest removal spectral weight. Because in interatomic *d-d* transitions leading to the ^2E_g removal state a change of the *d*-electron spin must occur upon electron addition to the minority spin e_g states, these transitions are expected to be weak. Thus, from the viewpoint of localized *d* electrons the interatomic transitions just across the insulating gap mainly happen via the transfer of minority spin t_{2g} electrons of one Ni site into the minority spin e_g states of an adjacent site.

As a consequence of this two-site process one would expect that feature *B* is absent in diluted octahedral Ni-O systems. In fact, this is observed by optical absorption on Ni-doped MgO crystals.[26] Since the Ni^{2+} ion is isolated in the MgO matrix without a neighboring Ni^{2+} ion, only the bandlike transition O $2p \rightarrow$Ni $3d$ can be excited as a low-energy excitation across the insulating gap. This excitation is observed in Ni:MgO at $\Delta E = 6.28$ eV, a value close to that of stoichiometric NiO.[9] The strong absorption edge that is seen in NiO ≈ 2 eV below the $2p \rightarrow 3d$ excitation energy and which should be due to the interatomic *d-d* transitions between adjacent Ni^{2+} ions, is not found in the Ni:MgO system and, thus, this result supports our two-site transition model.

The interpretation that a two-site process is causing the strong loss intensity just above the insulating gap is further supported by the different resonant behavior of features *A*, *B*, and *C* at the Ni $3s$ excitation threshold at $E_p = 102$ eV: Analogous to the mechanisms explained in Sec. IV leading to the enhanced excitation probability of the intra-atomic *d-d* transitions (feature *A*) at the threshold, also the *p-d* transitions (feature *C*) are resonantly enhanced at the threshold. Feature *B*, however—as expected for a two-site process—does not show a resonance at this energy.

According to calculations of optical properties of NiO (Ref. 27) features *C*, *D*, and *E* have been assigned to excitations of O $2p$ electrons. Peak *C* at 7.0-eV loss energy is caused by O $2p \rightarrow$Ni $3d$ transitions, feature *D* at 13.5 eV is due to O $2p \rightarrow$Ni $4s$ and feature *E* at 18 eV is due to O $2p \rightarrow$Ni $4p$ transitions. Peak *F* at 21.5 eV, the most intense feature at $E_p = 1200$ eV, is nearly completely missing at $E_p = 102$ eV. We assign loss peak *F* to the bulk plasmon excitation since its intensity decreases with a reduced bulk sensitivity of the measurement at lower primary energy (Fig. 1) or at grazing scattering geometry (not shown here). A similar behavior of plasmon losses is found on rare-earth oxides.[18,28] From the dielectric loss function $\mathrm{Im} -1/\epsilon(q,\omega)$ of NiO (Ref. 29) the possible plasma oscillation also can be inferred at $\Delta E = 22$ eV.

Within the gap region of NiO(100) (Fig. 1) only a very weak feature (*A*) is to be seen at $E_p = 1200$ eV while this and other weak peaks become more visible at lower primary energy. As will be discussed in Sec. IV, these weak structures are caused by intra-atomic *d-d* excitations.

The EELS spectra of CoO(100) (Fig. 1), taken at 370 K, exhibit—in analogy to NiO(100)—at high primary energy a gap region with weak features (*A*) caused by intra-atomic *d-d* transitions and the intense structure *C* due to O $2p \rightarrow$Co $3d$ transitions at 8.7 eV. BIS measurements on CoO(100) show very similar structures and peak positions compared to NiO(100) but a broader d^8 final-state peak due to its larger multiplet splitting.[30] The first affinity level $^3A_{2g}$ is calculated at 2.8 eV.[30] The energy position of the first $d^6\underline{L}^-$ ionization state of CoO seen in x-ray photoemission spectroscopy (XPS) (Ref. 30) is comparable to the position of the analogous state of NiO.

While the features above 12-eV loss energy in EELS are nearly identical for NiO(100) and CoO(100), it is at first sight surprising that the absorption edge is different. The much broader onset of the absorption edge in CoO(100) starts at 2.5 eV and has also been observed by optical-absorption measurements.[9] The major difference compared to the EELS curves of NiO(100) is that feature *B* is only barely visible at 6.3 eV for CoO(100). This is due to the much weaker probability of charge-transfer transitions in CoO. The ground state of Co^{2+} in CoO has $^4T_{1g}$ symmetry[30] with an electronic configuration $[(t_{2g}\uparrow)^3(e_g\uparrow)^2(t_{2g}\downarrow)^2]$ (Fig. 2) and the first electron addition state is of minority spin t_{2g} character. Since the first electron removal state is of intermediate spin character ($^3T_{1g}$), interatomic transitions of *d* electrons between two Co sites would involve the excitation of majority spin e_g electrons into minority spin t_{2g} states.[30] The transition rates for these processes are expected to be weak at high primary energy, even if the two Co sites are antiferromagnetically coupled. Transitions of minority spin t_{2g} electrons from one Co ion resulting in the $^5T_{2g}$ state into the empty minority spin t_{2g} states of an adjacent Co ion, however, are not forbidden by spin selection rules. The removal spectral weight in XPS is also the highest for the $^5T_{2g}$ state, which is at about 0.2 eV higher binding energy as the $^3T_{1g}$ state.[30] But nevertheless, these excitations do not lead to an intense feature in the EELS spectra. One reason for the weakness of the charge-transfer transitions in the spectra of CoO lies in the weaker mixing of *p*- and *d*-wave functions that appears with relaxation effects accompanying the intersite *d-d* transitions. Calculations of photoionized states[31] reveal that the mixing of ligand *p*-

hole states into d-hole states is weaker in CoO as compared to NiO. Due to the larger multiplet splitting of the d^8 final state the charge-transfer loss feature in CoO must additionally be broader, which is another reason for the less pronounced absorption edge in CoO. When the primary energy is lowered to $E_p = 100$ eV, the loss intensity of the charge-transfer transition between 2.5 and 8 eV is increased, which supports our assumption that relaxation processes are involved in the two-site transitions.

IV. INTRA-ATOMIC *d-d* EXCITATIONS IN NiO(100)

In this section, the loss structures within the gap region of NiO(100) are discussed. The experimental conditions have been varied in different ways to clarify if the loss structures are due to bulk or surface excitations and to reveal experimentally the influence of exchange interaction in the scattering process. Furthermore, the effect of the antiferromagnetic ordering on the *d-d* transition rates has been investigated. Figure 1 shows weak loss structures within the gap region of NiO(100), whose intensities are (relative to the intensity of the dipole allowed transition *B*) strongly enhanced with decreased primary energy. In Fig. 3, the gap structures of NiO(100) excited with low primary energies and measured in specular scattering geometry are shown with higher resolution. Their intensities (relative to feature *B*) increase with decreasing primary energy E_p and the 0.60-eV loss peak shows the strongest dependence. At $E_p = 102$ eV all loss structures are resonantly enhanced. Even with high resolution some of these gap features are no longer visible at primary energies of 1200 eV.[10]

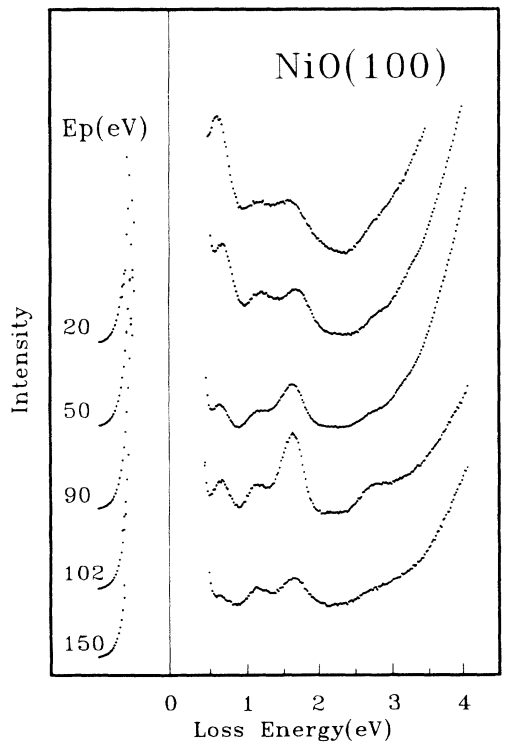

FIG. 3. Dependence of the gap structures of NiO(100) on the primary energy. The spectra were recorded in specular scattering geometry and show the gap intensity relative to the intensity of feature *B* (Fig. 1). Zero intensity is for each spectrum indicated by the bottom of the high-energy side of the elastic peak.

These gap structures (with the exception of the 0.60-eV loss) are caused by *intra-atomic* bulk excitations of electrons of the $3d^8$ configuration of one Ni^{2+} ion. Because of the different orientation of the d orbitals in the cubic lattice, the fivefold degenerate d orbitals of a free ion are split by the octahedral crystal field into threefold degenerate t_{2g} orbitals and twofold degenerate e_g orbitals. The energy splitting arises from an electrostatic term caused by the charges of the surrounding ligands and from a strong covalent term due to different overlapping of metal d-wave functions with ligand p-wave functions.[32] Upon excitation of these *intra-atomic d-d* transitions the change in the local charge density at the Ni site is small and, therefore, relaxation effects are negligible, which is in contrast to the case of *interatomic d-d* transitions. This allows the study of parity forbidden intra-atomic *d-d* transitions from the ground state with $^3A_{2g}$ symmetry to excited triplet and singlet states. Some of these excitations have previously been observed by optical absorption[13,14] and by EELS experiments on polycrystalline samples,[33] polished crystals,[34] and thin films of NiO.[35]

A. Influence of the primary energy

The loss peak at 0.60 eV has not been observed in optical absorption[13,14] and it cannot be seen in the EELS curves of Cox and Williams.[34] It has also been found in thin NiO(100) films by Freitag *et al.*,[35] who attributed the loss peak to a surface state. As has been suggested previously,[10] the occurrence of the 0.60-eV peak on cleaved NiO(100) crystals is also due to the excitation of a surface state. EELS measurements at $E_p = 50$ eV reveal directly after the cleavage of the crystal an intense loss peak at 0.60 eV; its intensity is strongly reduced within several hours at a current density of the primary beam lower than 0.2 μA/mm^2. The surface peak at 0.60 eV remains visible, however, several days at these conditions. At higher current densities the surface peak vanishes completely whereas the other bulk structures inside the gap remain nearly unchanged. When the surface sensitivity of the experiment is altered by using different scattering geometries, a drastic change in intensity of the surface peak can be observed (Fig. 4, $E_p = 102$ eV). The very strong enhancement of the scattering cross section for the surface transition at low primary energies and its vanishing cross section at high primary energies[10] is a clear indication of a parity forbidden process. This suggests that the surface state is of d character. Defect states are not causing the 0.60-eV peak since it is absent in samples sputtered with Ar^+ ions (500 eV), which usually have a higher defect concentration at the surface. Cluster calculations of *d-d* excitation energies in NiO(100) (Ref. 35) show that the lower symmetry of the crystal field at the surface (C_{4v}) leads to a partial lifting of the degeneration of the $^3T_{2g}$ excited bulk state. At the surface the $^3T_{2g}$ state, which is found experimentally at 1.12 eV, splits into the ^{3}E component calculated at 0.62 eV and the $^3B_2$ component calculated at 0.98 eV. We, therefore, attribute the 0.60 eV loss peak to the transition

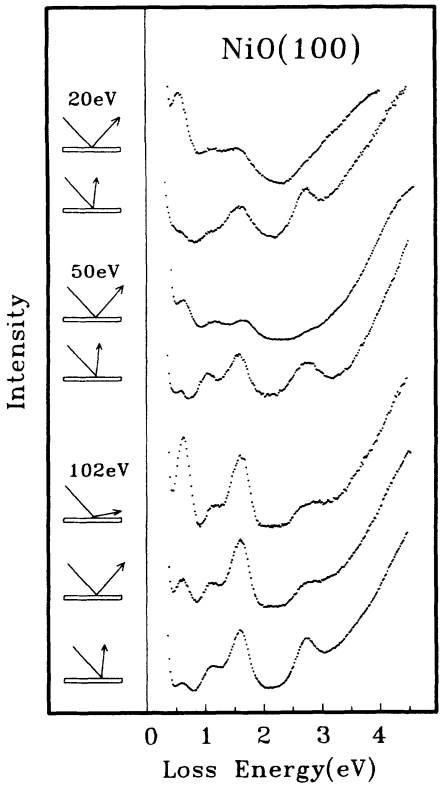

FIG. 4. Dependence of the gap structures of NiO(100) on the scattering angle. The spectra were recorded specularly with 90° scattering angle relative to the primary direction or with 125° scattering angle in off-specular geometry. At $E_p = 102$ eV an additional curve with 65° scattering angle is inserted.

$^3A_{2g} \rightarrow {}^3E$ at the surface. Further support of the surface character of the 0.60-eV peak is obtained by adsorption measurements: When NO molecules are adsorbed at the (100) surface of a thin film of NiO the stronger ligand field component normal to the surface shifts the ^3E component to higher energies.[35]

Whereas the visibility of the ^3E surface component is strongly dependent on the surface sensitivity of the measurement (Fig. 4), there appears no analogous change in intensity of the 1.12-eV loss peak, which should be a superposition of the $^3T_{2g}$ bulk loss and $^3B_2$ surface loss component. Therefore, transitions to the $^3B_2$ surface state seem to have much weaker excitation probabilities than transitions to the ^3E state. This finding is in agreement with the experimental results of Freitag *et al.*[35] However, when the ^3E surface state is reduced after prolonged electron irradiation or by sputtering of the sample, the intensity of the 1.12-eV loss is also slightly decreased. This can be the consequence of the reduction of the $^3B_2$ surface loss component. The calculated splitting of the $^3T_{1g}$ bulk state[35] at the surface into the $^3A_2$ and ^3E states could not be observed in this EELS experiment.

One EELS spectrum measured at grazing exit of the scattered electrons additionally showed a weak loss peak at 2.1 eV. At this energy position previous optical-absorption spectra[13,14] exhibit a shoulder that remained unexplained. We assume that this peak is due to defect states because this peak is also present in EELS spectra of sputter-annealed samples.[36]

A compilation of experimental and theoretical data for *d-d* transition energies for NiO(100) is given in Table I. The data of Fujimori and Minami[24] and van Elp *et al.*[25] have been obtained from parameters of calculated PES curves and the data of Freitag *et al.*[35] are taken from *ab initio* configuration interaction cluster calculations. A comparison of measured *d-d* transition energies from optical absorption[13,14] with our values and those from EELS on single crystals[34,36] shows that the transitions $^3A_{2g} \rightarrow {}^3T_{2g}, {}^1E_g$ are observed at lower excitation energies with EELS.

As can be inferred from Fig. 3 and our previous high-energy EELS measurements,[10] the scattering cross sections of individual *d-d* transitions depend in specular scattering geometry differently on the primary energy. Since *d-d* transitions are in centrosymmetric environments forbidden by the parity selection rule as electric-dipole transitions, their scattering cross section is very weak for photons and for electrons of high primary energy. If observed with photons, the intensity of *d-d* transitions mainly arises from electric-dipole transitions that become allowed by the presence of odd-parity fields caused by nuclear displacements in the cubic lattice and by lattice vibrations, which slightly release the parity selection rule.[32] With electrons of low energy, *d-d* transitions can additionally be excited by electron exchange.

Compared to the parity forbidden triplet-triplet *d-d* transitions, which can be excited by direct scattering as well as by exchange scattering, the triplet-singlet *d-d* transitions are additionally forbidden by spin selection rules and cannot be excited by dipole scattering, since the dipole operator has in the absence of spin-orbit coupling no matrix elements between states of different spin multiplicities. Therefore, we expect that effects of exchange scattering in EELS measurements with unpolarized primary electrons should be visible best for multiplicity changing transitions.

The strong dependence on the primary energy of the probability for electron exchange scattering is used for

TABLE I. Ground state and final states of intra-atomic *d-d* transitions in NiO(100). Their corresponding excitation energies have been measured with this EELS experiment and optical absorption (Refs. 13 and 14) or have been calculated (Refs. 25, 24, and 35). Energies are in eV.

Symmetry	EELS	Opt. Abs.		Theory		
$^3A_{2g}$	0	0		0		
^3E	0.60					0.62
$^3T_{2g}$	1.12	1.13	1.08	1.22	1.12	1.00
^1E_g	1.60	1.75	1.73	1.68	1.92	
$^3T_{1g}$	1.70	1.95	1.88	1.98	1.88	1.81
$^1A_{1g}$		3.25		2.64	3.10	
$^1T_{2g}$	2.75	2.75	2.73	3.00	3.03	
$^3T_{1g}$	2.9	2.95	2.95	3.37	3.23	
$^1T_{1g}$	3.1	3.52	3.26	3.49	3.60	

the 1.60-eV loss feature to clarify its attribution either to the ${}^3A_{2g} \rightarrow {}^3T_{2g}$ or to the ${}^3A_{2g} \rightarrow {}^1E_g$ transition because the calculated energies for the triplet-triplet and triplet-singlet excitations do not coincide (see Table I). Our EELS spectra exhibit at $E_p = 102$ eV a peak at 1.60 eV and a shoulder at 1.70 eV. Therefore, this loss complex is due to at least two excitation channels. The peak position is shifted to 1.70 eV at primary energies of 500 and 1200 eV and the shoulder disappears.[10] We explain this by the strong decrease of the excitation channel at 1.60 eV with increasing primary energy and we attribute the 1.60-eV loss to the ${}^3A_{2g} \rightarrow {}^1E_g$ transition excited by exchange scattering. We emphasize that in analogy to this the very strong dependence of exchange scattering on the primary energy has been reported previously for an exchange f-f transition in a rare-earth oxide.[18]

The strong enhancement of the d-d loss intensity with decreasing primary energy (Figs. 1 and 3) also explains why Kemp, Davies, and Cox[33] found such discrepancies in a comparison of the d-d loss peak intensities of CoO, NiO, and other oxides measured by optical absorption and with EELS at $E_p = 20$ eV.

Our measurements suggest that exchange scattering of localized $3d$ electrons in NiO plays an important role even at primary energies much higher than the loss energy. Opposite to exchange scattering on simple atoms such as He, where the scattering cross section becomes largest when primary energy E_p and loss energy ΔE are nearly equal and where the cross section is negligible for $E_p/\Delta E \geq 10$,[37] the hybridization of the localized states with bandlike states can lead in solids to a different dependence of these exchange processes on the primary energy. It seems, however, that exchange scattering of localized low-energy electrons in NiO and CoO plays an important role even at primary energies with $E_p/\Delta E \approx 50$. Similar results can be obtained from spin-forbidden f-f transitions in Yb_2O_3 (Ref. 18) and in gadolinium, where in a similar EELS experiment f-f transitions are observed with high intensity at $E_p = 120$ eV.[16]

The only inelastic scattering channel within the gap of NiO(100) that still grows in intensity even at very low primary energies, is the excitation of the surface d-d transition at 0.60 eV (Fig. 3). While this transition is not observable at $E_p = 1200$ eV (Ref. 10) due to the low surface sensitivity and the low scattering cross section, it leads to the most intense loss feature in the gap at low primary energy. At $E_p = 8$ eV (not shown here) it shows twice the intensity as at $E_p = 20$ eV although the penetration depth of the electrons into the bulk is higher. Hence it follows that the increase of the scattering cross section is so intense that the expected decrease of loss intensity due to the lower surface sensitivity is compensated. This surface d-d excitation exhibits a behavior that is found in exchange scattering on atoms or in the excitation of bulk states with very low hybridization.

In Fig. 3, all gap structures appear enhanced at $E_p = 102$ eV. A careful analysis shows a resonant enhancement of all d-d excitations between $E_p = 100$ eV and $E_p = 105$ eV with the maximum at 103 eV (Ref. 38) due to a process at the Ni $3s$ threshold similar to those observed by appearance potential spectroscopy on rare-earth compounds.[39] When the primary energy is just sufficient to excite a Ni $3s$ electron, both primary and excited core electron can intermediately be captured in a $3d$ state ($3s^2 3d^8 + e^- \rightarrow 3s^1 3d^{10}$). This intermediate state can decay ($3s^1 3d^{10} \rightarrow 3s^2 3d^{8*} + e^-$) via Super Coster Kronig transitions into an excited $3d^{8*}$ state with emission of an electron with energy $E_P - \Delta$ (Δ is the d-d excitation energy). Since the same excited $3d^{8*}$ state can also be reached by exchange scattering with energy loss Δ of the scattered electron, both excitation channels can interfere and enhance the d-d transition probability. In the EELS experiment the excitation threshold is lowered several eV due to the strong interaction between the core hole and the captured electron in a d state. In PES on NiO(100) the occurrence of a resonance some eV below the atomic Ni $3s$ excitation threshold has also been observed.[40]

B. Influence of the scattering geometry

Another way of probing the influence of direct and exchange scattering mechanisms on the d-d transition rates is the variation of the scattering geometry. Figure 4 reveals the drastic influence of the scattering angle of the electrons on the EELS curves. The scattering angle is defined as the angle between the direction of the analyzed scattered beam and the direction of the primary beam, which is kept constant at 45° off the surface normal.

Whereas the change in the surface sensitivity with different scattering angles at fixed primary energy is the decisive factor for the observed intensity changes of the surface peak at 0.60 eV, it is primarily the scattering angle-dependent excitation cross section that causes the observed intensity of bulk d-d transitions. At lower primary energies the intensity of the 1.60-eV peak, attributed to the ${}^3A_{2g} \rightarrow {}^1E_g$ transition, is raised against the 1.12-eV peak (${}^3A_{2g} \rightarrow {}^3T_{2g}$) at higher scattering angles. A strong intensity enhancement at increased scattering angles also occurs at low primary energies at the 2.75-eV loss, which is only weakly visible in specular geometry. This loss is attributed to the ${}^3A_{2g} \rightarrow {}^1T_{2g}$ transition. No dependence on the scattering angle has been found for the loss intensity of the ${}^3A_{2g} \rightarrow {}^3T_{1g}$ transitions at 1.70 and 2.9 eV.

EELS spectra at $E_p = 102$ eV that were taken at a constant off-specular scattering angle but with different incident angles of the primary electrons (not shown here) show similar relative intensities of the bulk peaks although the difference between the exit angle of the scattered electrons and the angle of the specularly reflected electrons is changed. This would support the interpretation of Matthew *et al.*[16] that one observes with EELS in reflection geometry not only inelastic losses with low-momentum transfer preceded or followed by high angle elastic scattering, but also large angle inelastic scattering for electron exchange processes. Since the scattering cross sections of dipole allowed excitations and exchange excitations depend differently on the scattering angle, exchange processes are better observable in off-specular

scattering geometry.[16] Whereas the cross section for dipole excitations peaks sharply in specular geometry because of the low-momentum transfer involved in dipole transitions, the intensity of exchange excitations of localized low-energy states in solids is spread out over a wider angular range due to the higher-momentum transfer.

Therefore, the strong increase of the 1.60-eV peak at larger scattering angles additionally supports its interpretation as the spin-forbidden $^3A_{2g} \rightarrow {}^1E_g$ transition. Also the analogous behavior of the 2.75-eV peak at different scattering angles is an indication of the $^3A_{2g} \rightarrow {}^1T_{2g}$ spin-forbidden process. At $E_p = 1200$ eV we found that the intensity of the $^3A_{2g} \rightarrow {}^1T_{2g}$ transition is not increased at higher scattering angles. This is due to the vanishing exchange contribution to this transition at higher primary energies.

C. Influence of the antiferromagnetic ordering

NiO is antiferromagnetic below the Néel temperature of 523 K.[41] The magnetic moments are oriented parallel within one (111) plane and point into the antiparallel direction within the adjacent (111) plane.[42] Due to the superexchange interaction of the *d* electrons in neighboring (111) planes, the simple cubic lattice of NiO is rhombohedrally distorted below the Néel temperature. In calculations of the band structure of NiO the inclusion of antiferromagnetic ordering is essential for the appearance and the nature of the insulating gap,[21,43] whereas EELS measurements at room temperature and at the Néel temperature reveal no changes for the transition across the insulating gap.[10]

In Fig. 5, a comparison of an EELS spectrum of NiO(100) taken at room temperature, where the long-range magnetic ordering exists nearly completely, and a spectrum taken just above the temperature of the Néel point is given. At 525 K the intensities of the bulk excitations within the insulating gap are lowered and the peaks are broadened. After cooling down to room temperature the intensities of the bulk loss peaks appear exactly as before the heating. The strong decrease of the surface peak at 525 K is, however, an irreversible change. After cooling to room temperature its intensity remains very weak.

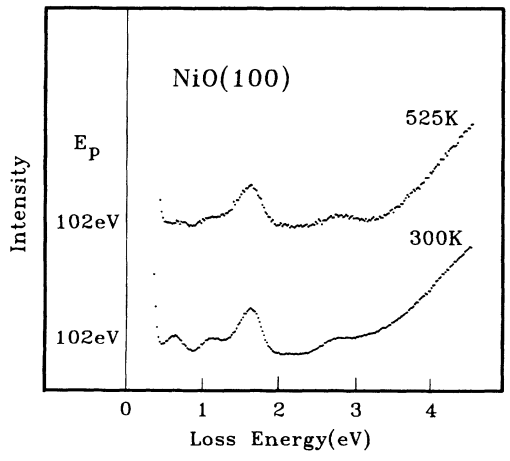

FIG. 5. Dependence of the gap structures of NiO(100) on the temperature. The spectra were recorded at room temperature and just above the Néel temperature.

Since an explanation of this effect by adsorption of molecules on the sample surface during the measurement can be ruled out and since a decomposition of the sample at the Néel temperature would produce defect states within the gap, which are not observed, we assume that the decrease of the surface peak at the Néel point is caused by a change of the electronic structure at the surface. This intensity reduction of the surface peak has not been observed when NiO(100) samples were heated several days only to 380 K, whereas at 525 K the intensity is reduced within several hours. The exact temperature of the appearance of the observed surface change cannot be given at present and, therefore, the possible influence of the antiferromagnetic ordering cannot be estimated.

The weak visibility of the spin-forbidden transition $^3A_{2g} \rightarrow {}^1E_g$ even in optical spectroscopy has been attributed to the antiferromagnetic ordering in NiO.[14,19] In optical absorption of MgO:Ni samples one observes an increasing intensity ratio of the $^3A_{2g} \rightarrow {}^1E_g$ to the $^3A_{2g} \rightarrow {}^3T_{2g}$ transitions with higher Ni concentration, which is probably due to the higher degree of magnetic coupling.[19] A similar enhancement of the triplet-singlet excitations with higher Ni doping has been proposed by Bird.[20]

However, in our EELS spectra of undoped NiO(100) no change of the 1.60-eV loss peak shape (except for a broadening) appears by raising the sample temperature to the Néel point, so that there seems to be only little influence of the antiferromagnetism on the relative transition rates of the different excitation channels. We emphasize that our measurements have been taken at $E_p = 102$ eV, where *d-d* transitions are resonantly enhanced. Even with EELS on resonance, the loss spectra are apparently not influenced by the long-range magnetic ordering of the magnetic moments in NiO. Some mechanisms like short-range magnetic ordering that still persists above the Néel point would explain this. From spin-polarized diffraction measurements at antiferromagnetic MnO a short-range magnetic order is inferred up to 4.5 times the Néel temperature.[44] EELS measurements over a more extended temperature interval would, therefore, be highly desirable.

V. INTRA-ATOMIC *d-d* TRANSITIONS IN CoO(100)

All EELS spectra on cleaved CoO(100) have been measured at 370 K to avoid a charging of the surface. This temperature is well above the Néel temperature $T_N = 289$ K of CoO.[41] In CoO the ^4F ground-state of the free Co^{2+} ion is split into states with $^4T_{1g}$, $^4T_{2g}$, and $^4A_{2g}$ symmetry. The ground state of Co^{2+} in CoO with the electronic configuration $[(t_g\uparrow)^3(e_g\uparrow)^2(_{2g}\downarrow)^2]$ (Fig. 2) has $^4T_{1g}$ symmetry.[30]

In Fig. 1, the loss features due to transitions to excited quartet and doublet levels within the insulating gap of CoO(100) are shown. Figure 6 shows these structures with higher resolution. The intensities of the two peaks

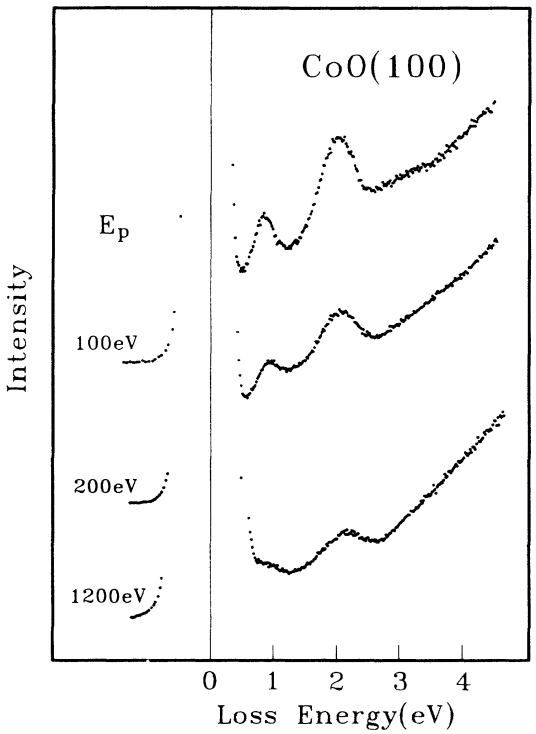

FIG. 6. Dependence of the gap structures of CoO(100) on the primary energy. The spectra were recorded in specular scattering geometry and show the gap intensity normalized to the intensity of feature C in CoO(100) at the corresponding primary energy (Fig. 1). Zero intensity is for each spectrum indicated by the bottom of the high energy side of the elastic peak.

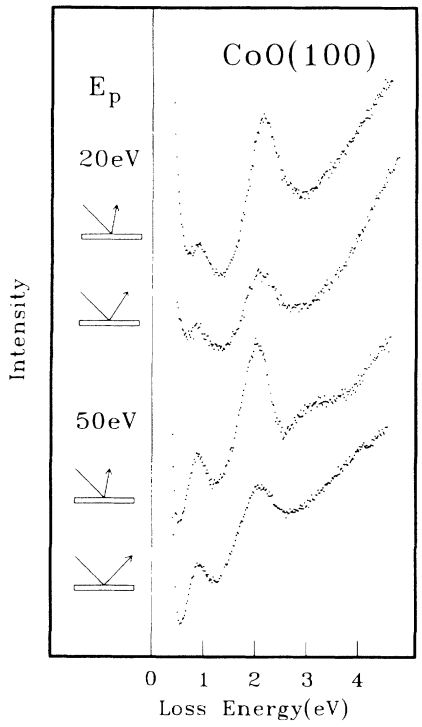

FIG. 7. Dependence of the gap structures of CoO(100) on the scattering angle. The spectra were recorded specularly with 90° scattering angle relative to the primary direction or with 125° scattering angle in off-specular geometry.

at 0.85 and 2.05 eV are normalized to the intensity of the dipole allowed feature C at the corresponding primary energy. Both gap structures depend similarly on the primary energy as the corresponding bulk d-d transitions in NiO(100) do: At high primary energy the gap structures are very weak and their intensities increase strongly at lower primary energies. At $E_p = 1200$ eV the peak position of the second feature is shifted to 2.25 eV. Analogous structures within the gap of CoO have also been found previously by optical absorption[15] and EELS on polycrystalline samples.[33]

The peak at 0.85 eV is attributed to the transition ${}^4T_{1g} \rightarrow {}^4T_{2g}$. The 2.05-eV peak is composed of several unresolved structures: Whereas the spin-forbidden quartet-doublet excitation ${}^4T_{1g} \rightarrow {}^2T_{1g}$ can only be seen as a weak shoulder at 2.04 eV in optical measurements at the temperature of liquid nitrogen and is not visible at room temperature due to the broadening of the lines,[15] it leads in EELS at low primary energies to a pronounced loss feature at 2.05 eV due to exchange scattering. The transition ${}^4T_{1g} \rightarrow {}^4T_{1g}$ which has been observed at 2.3 eV with photons is in EELS better visible at high primary energy because the scattering cross section of the quartet-doublet exchange transition falls off rapidly at higher primary energies. This leads to the observed shift in the mean peak position of the overlapping loss features. Further confirmation of the strong exchange scattering contribution to the ${}^4T_{1g} \rightarrow {}^2T_{1g}$ transition is the enhanced peak intensity at higher scattering angles in off-specular scattering geometry (Fig. 7). As in the case of NiO(100), excitations involving a change in the spin multiplicity are better observable at higher scattering angles.

The broad and weak feature at about 3.2-eV loss energy could be due to the transition ${}^4T_{1g} \rightarrow {}^4A_{2g}$. This transition is expected to be weak since it is a two-electron excitation $t_{2g}^5 e_g^2 \rightarrow t_{2g}^3 e_g^4$. The 3.2-eV feature can be observed directly after the cleavage of the CoO crystal. It is, however, very difficult to make a reliable assignment of this feature because the EELS data of some CoO(100) samples exhibited changes during the measurements that resulted in a strong peak at 3 eV. If this electron-beam-induced 3-eV feature is due to the presence of defect states created by the measurements or due to the formation of Co_3O_4, as might be inferred from our BIS data, is open at present.

EELS measurements could not be performed below the Néel temperature of CoO. According to the results on NiO(100) we expect that the influence of antiferromagnetic ordering is also weak in CoO. Such distinct indications of the existence of a surface d state, which have been found at NiO(100), cannot be found at CoO(100). A comparison of our experimental values with the theoretical predictions for d-d transition energies in CoO (Ref. 30) is given in Table II.

TABLE II. Ground state and final states of intra-atomic *d-d* transitions in CoO(100). Their corresponding excitation energies have been measured with this EELS experiment and optical absorption (Ref. 15) or have been calculated (Ref. 30). Energies are in eV.

Symmetry	EELS	Opt. Abs.	Theory
$^4T_{1g}$	0	0	0
^2E_g			0.73
$^4T_{2g}$	0.85	0.9–1.04	1.07
$^2T_{1g}$	2.05	2.04	1.92
$^2T_{2g}$		2.06	2.46
$^4T_{1g}$	2.25	2.3	2.68
$^4A_{2g}$	3.2 ?	2.15	3.06

VI. CONCLUSIONS

We have shown the strong influence of the primary energy and the scattering geometry on the EELS spectra of NiO(100) and CoO(100). The observed excitations involving 3*d* electrons can be well interpreted in a localized picture of the 3*d* states. As the cause of the strong loss intensity just above the insulating gap of NiO we found interatomic *d-d* transitions between adjacent TM ions that involve strong relaxation effects due to the large change in the local charge density of the *d* orbitals. For the intra-atomic *d-d* crystal-field excitations relaxation effects are negligible and consequently the parity forbidden *d-d* transitions are observed at high primary energies only as very weak structures within the insulating gap of both oxides. With EELS at low energies the forbidden *d-d* transitions appear strongly enhanced because of electron exchange scattering. Exchange scattering plays a dominant role for triplet-singlet transitions in NiO(100) and quartet-doublet transitions in CoO(100); it is suggested that large angle inelastic scattering contributes strongly to the observed excitations. On NiO(100) a surface state has been found that is identified as a *d* state. The excitation probability of the surface *d-d* transition in NiO(100) depends most strongly on the primary energy. The intensity increases steadily when the primary energy approaches the loss energy. When the primary energy reaches the Ni 3*s* excitation threshold in NiO, the intensity of the forbidden *d-d* transitions is resonantly enhanced. Triplet-triplet and triplet-singlet excitations in NiO(100) are not differently influenced by the antiferromagnetic ordering. Due to the localized character of the exchange excitations in both oxides we would expect strong spin-dependent effects in scattering primarily spin-polarized electrons.

ACKNOWLEDGMENTS

We would like to thank A. Scheipers, C. Henig, and B. Fromme for their valuable contributions in the course of this work. We thank V. Staemmler for sending us the results of his cluster calculations for NiO(100) prior to publication. The financial support from the Deutsche Forschungsgemeinschaft is gratefully acknowledged.

[1]P. A. Cox, *Transition Metal Oxides* (Clarendon, Oxford, 1992).
[2]V. E. Henrich, Rep. Prog. Phys. **48**, 1481 (1985).
[3]J. Zaanen, G. A. Sawatzky, and J. W. Allen, Phys. Rev. Lett. **55**, 418 (1985).
[4]G. A. Sawatzky, in *Core-Level Spectroscopy in Condensed Systems*, edited by J. Kanamori and A. Kotani (Springer-Verlag, Berlin, 1988).
[5]B. H. Brandow, Adv. Phys. **26**, 651 (1977).
[6]N. F. Mott, Proc. Phys. Soc. London Sect. A **62**, 416 (1949).
[7]J. Hubbard, Proc. R. Soc. London Ser. A **277**, 237 (1964).
[8]S. Hüfner, P. Steiner, I. Sander, M. Neumann, and S. Witzel, Z. Phys. B **83**, 185 (1991).
[9]R. J. Powell and W. E. Spicer, Phys. Rev. B **2**, 2182 (1970).
[10]A. Gorschlüter and H. Merz, Int. J. Mod. Phys. B **7**, 341 (1993).
[11]K. Terakura, A. R. Williams, T. Oguchi, and J. Kübler, Phys. Rev. Lett. **52**, 1830 (1984).
[12]S. Hüfner, P. Steiner, I. Sander, F. Reinert, and H. Schmitt, Z. Phys. B **86**, 207 (1992).
[13]R. Newman and R. M. Chrenko, Phys. Rev. **114**, 1507 (1959).
[14]V. Propach, D. Reinen, H. Drenkhahn, and Hk. Müller-Buschbaum, Z. Naturforsch. Teil B **33**, 619 (1978).
[15]G. W. Pratt and R. Coelho, Phys. Rev. **116**, 281 (1959).
[16]J. A. D. Matthew, W. A. Henle, M. G. Ramsey, and F. P. Netzer, Phys. Rev. B **43**, 4897 (1991).
[17]F. Della Valle and S. Modesti, Phys. Rev. B **40**, 933 (1989).
[18]A. Gorschlüter, R. Stiller, and H. Merz, Surf. Sci. **251/252**, 272 (1991).
[19]D. Reinen, Ber. Bunsenges. Phys. Chem. **69**, 82 (1965).
[20]B. D. Bird, G. A. Osborne, and P. J. Stephens, Phys. Rev. B **5**, 1800 (1972).
[21]M. Belkhir and J. Hugel, Solid State Commun. **70**, 471 (1989).
[22]K. Jost, J. Phys. E **12**, 1006 (1979).
[23]NiO and CoO single crystals have been produced by Earth Jewelry Co., Ltd., Osaka, Japan.
[24]A. Fujimori and F. Minami, Phys. Rev. B **30**, 957 (1984).
[25]J. van Elp, H. Eskes, P. Kuiper, and G. A. Sawatzky, Phys. Rev. B **45**, 1612 (1992).
[26]K. W. Blazey, Physica **89B**, 47 (1977).
[27]J. Hugel and M. Belkhir, Solid State Commun. **73**, 159 (1990).
[28]E. Bertel, F. P. Netzer, and J. A. D. Matthew, Surf. Sci. **103**, 1 (1981).
[29]S. Suga, K. Inoue, M. Taniguchi, S. Shin, M. Seki, K. Sato, and T. Teranishi, J. Phys. Soc. Jpn. **52**, 1848 (1983).
[30]J. van Elp, J. L. Wieland, H. Eskes, P. Kuiper, G. A. Sawatzky, F. M. F. de Groot, and T. S. Turner, Phys. Rev. B **44**, 6090 (1991).
[31]G. Grenet, Y. Jugnet, T. M. Duc, and M. Kilber, J. Chem. Phys. **74**, 2163 (1981).
[32]C. J. Ballhausen, *Introduction to Ligand Field Theory* (McGraw-Hill, New York, 1962).
[33]J. P. Kemp, S. T. P. Davies, and P. A. Cox, J. Phys. Condens. Matter **1**, 5313 (1989).
[34]P. A. Cox and A. A. Williams, Surf. Sci. **152/153**, 791 (1985).
[35]A. Freitag, V. Staemmler, D. Cappus, C. A. Ventrice, K. Al Shamery, H. Kuhlenbeck, and H.-J. Freund, Chem. Phys.

Lett. **210**, 10 (1993).
[36]B. Fromme (private communication).
[37]G. F. Hanne, Phys. Rep. **95**, 95 (1983).
[38]A. Gorschlüter and H. Merz (unpublished).
[39]H. Hinkers, R. Stiller, and H. Merz, Phys. Rev. B **40**, 10 594 (1989).
[40]H. Kuhlenbeck, G. Odörfer, R. Jaeger, G. Illing, M. Menges, Th. Mull, H.-J. Freund, M. Pöhlchen, V. Staemmler, S. Witzel, C. Scharfschwerdt, K. Wennemann, T. Liedtke, and M. Neumann, Phys. Rev. B **43**, 1969 (1991).
[41]J. Kübler and A. R. Williams, J. Magn. Magn. Matter **54-57**, 603 (1986).
[42]W. L. Roth, J. Appl. Phys. **31**, 2000 (1960); G. A. Slack, *ibid.* **31**, 1571 (1960).
[43]Z. X. Shen, R. S. List, D. S. Dessau, B. O. Wells, O. Jepsen, A. J. Arko, R. Barttlet, C. K. Shih, F. Parmigiani, J. C. Huang, and P. A. P. Lindberg, Phys. Rev. B **44**, 3604 (1991).
[44]B. Hermsmeier, J. Osterwalder, D. J. Friedman, and C. S. Fadley, Phys. Rev. Lett. **62**, 478 (1989).